Journal of Power Sources 625 (2025) 235623

Contents lists available at ScienceDirect

Journal of Power Sources

journal homepage: www.elsevier.com/locate/jpowsour

The performance of biochar waste-derived electrodes in different bio-electrochemical applications

Andrea Goglio [a], Arianna Carrara [a], Hager Galal Elsayed Elboghdady [a], Mirko Cucina [b], Elisa Clagnan [a], Gabriele Soggia [a], Patrizia De Nisi [a], Fabrizio Adani [a,*]

[a] Gruppo Ricicla Lab., Department of Agricultural and Environmental Science, University of Milan, Via Celoria 2, 20133, Milan, Italy
[b] National Research Council of Italy, Institute for Agriculture and Forestry Systems in the Mediterranean (ISAFOM-CNR), Via Della Madonna Alta 128, 06128, Perugia, Italy

HIGHLIGHTS

- Organic wastes can be transformed by bioelectrochemical systems (BES) in useful products.
- Biochar can be used producing low-cost cathode reducing BES cost.
- Kitchen waste (OW) and wood chips (WC) biochar were used for cathode production.
- WC-based electrodes performed better than OW-based ones.
- BET surface and graphite-like structure explained electrode good performance.

GRAPHICAL ABSTRACT

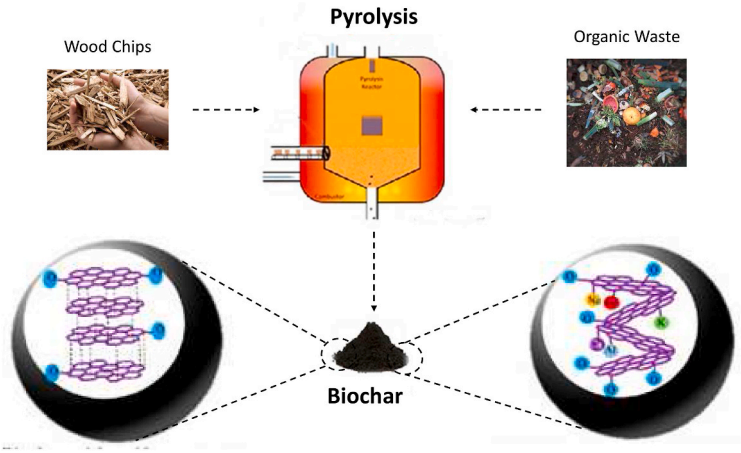

ARTICLE INFO

Keywords:
Biochar-based electrode
CO_2 electro-recycling
Microbial electrosynthesis
Microbial fuel cell
Microbial electrolysis cell
Organic wastes

ABSTRACT

This work studied the performances of two *ad hoc* biochar-based cathode materials: one obtained from pyrolysis of the organic fraction of municipal solid waste (OW) and the other of wood chips (WC), in the context of three different bio-electrochemical reactors' scope: MFC, MEC and MES. Cathodes were characterized through composition, pH, specific surface area and infrared spectroscopy; then production of electricity, methane (CH_4), and volatile fatty acids (VFAs) from carbon dioxide (CO_2) was described, and finally the microbial community was explored through 16S rRNA gene sequencing. WC-based electrodes performed better than OW-based ones. WC (200 ± 25 mV) generated twice the amount of electricity compared to OW (100 ± 10 mV) in MFC modality. In MEC modality, WC achieved both higher CH_4 production and concentration (3.6 ± 0.7 mL per day, 73.2 ± 3.9 % v/v, respectively) than OW (3.0 ± 0.3 mL per day, 70 ± 8 % v/v, respectively). In MES modality, WC produced ten times more acetic acid (0.3 ± 0.13 g L^{-1} per day) than OW (0.03 ± 0.04 g L^{-1} per day). The better performance of the WC-biochar cathode was attributed to its higher Brunauer–Emmett–Teller (BET) value and its

* Corresponding author.
E-mail address: fabrizio.adani@unimi.it (F. Adani).

https://doi.org/10.1016/j.jpowsour.2024.235623
Received 12 February 2024; Received in revised form 21 June 2024; Accepted 14 October 2024
Available online 29 October 2024

carbonaceous graphite-like structure. NGS analysis highlighted the presence of specific genera of microorganisms leading to the differential functioning of the systems.

1. Introduction

The production of energy and chemicals demands a high consumption of fossil fuels, inevitably leading to the depletion of non-renewable resources, waste generation, greenhouse gases (GHGs) emissions and environmental pollution [1]. These consequences have prompted new research on renewable fuels and low-carbon raw materials.

Carbon dioxide is the primary GHG generated by human activities [2]. The global concentration of CO_2 in the atmosphere increased from 10 to almost 40 Gt from the second half of the 1900s until 2020 with a significant reduction only during the COVID-19 pandemic (Global Carbon Project, 2020). Statistical models forecast that by 2100, CO_2 amount in the atmosphere will range between 54 Gt and 97 Gt [3]. The combustion of fossil fuels for industrial and chemical purposes is largely responsible for CO_2 emissions [4,5]. An average increase of between 1.1 and 6.4 °C the Earth's temperature is expected by the end of the 21st century, due to GHGs' accumulation [3]. The linear economic model is therefore not sustainable in the long run, and a new circular approach is required to meet the growing energy demand [6]. The development and improvement of new technologies for the production of renewable energy is necessary. Availability, conversion efficiency, and utilization of natural resources play a critical role in the transition to a circular economy model. Challenges related to the intermittency (storage rate and volume) of power generation also need to be addressed [7].

An alternative to fossil-based fuels is biomass, which can be used as a feedstock in the processes that generate bioenergy, including biofuels and biogas, as well as various bio-based chemicals [8]. Worldwide, the production of biofuels and biomaterials from biomass is on the rise (Statistical Review of World Energy, 2022). However, there are environmental concerns regarding land competition with food production, water usage, and land transformation [9].

In this context, bioelectrochemical systems (BES), which include microbial fuel cells (MFCs), microbial electrolytic cells (MECs) and microbial electrosynthesis cells (MESs), are one group of candidates to lead the ecological transition. BESs are capable of converting organic wastes into electricity, hydrogen or other chemical products by electrochemical reduction processes. Their design consists of an anode where oxidation occurs and a cathode where reduction occurs, and at least one of these reactions is microbially catalyzed [10]. MFCs generate bioelectricity from wastewater and other sources [11,12]. MECs oxidize organic matter and produce hydrogen (H_2) and/or methane (CH_4) using relatively low energy input [13,14]. MESs convert CO_2 and water into multi-carbon extracellular organic compounds, such as volatile fatty acids (VFAs) which can be further used for bioplastic production, or other valuable biobased compounds [15–17].

One of the major challenges of MFCs is related to the oxygen reduction reaction (ORR) on carbon-based electrodes, which negatively affects cathode performance [18]. A high cathode overpotential generally indicates slow ORR at standard ambient conditions, i.e. temperature of 298.15 K and pressure of 100 kPa [19]. A carbonaceous air biocathode can function without chemical catalysts. For example, performances at the laboratory scale have been analyzed on cathodes composed only by a cylindrical electrode of 100 % biochar [20] with a further comparison of different uses of biochar from laboratory to real scale better describing the applications of biochar as a cathode [21]. However, to enhance the reaction and reduce cathode overpotential, electrocatalysts like Pt-C, though expensive, have been used [22]. Low-cost electrocatalysts, such as biomass-derived black carbon materials (biochar), are being explored as solutions, given their cost-effectiveness and remarkable properties for ORRs, including high surface area, trace metal content, high porosity, biocompatibility, and high conductivity [23,24].

In the case of MESs, various factors, such as operating conditions, pH, temperature, membrane characteristics, and cathode potential and material, influence their performance [16]. Cathode materials play a critical role in electricity-driven CO_2 reduction by microorganisms [25]. Two-dimensional (2D) carbon-based materials, like carbon cloth or carbon felt, are used as cathodes due to their better electrical conductivity, stability, light weight, flexibility, and higher porosity compared to graphite electrodes [25] than 3D materials. On the other hand, 2D carbon-based materials have lower volumes of reactive surface area for the attachment and growth of microbial (mainly bacterial and archaeal) biomass because of differences in the material structural organization [26]. Therefore, they exhibit reduced mass and electron transfer compared to 3-dimensional materials such as carbon felt and carbon fiber rods [26].

These systems are currently being studied at the laboratory scale, so their implication in energy transition is still challenging. This experiment, even though carried out at a laboratory scale with a technology readiness level (TRL) of 4, aims to be an initial exploratory experiment focused on providing guidelines to facilitate the scaling up of the process by gradually increasing its scale and, consequently, TRL. More specifically, two distinct biochar-based electrodes were created, both produced from waste biomass: 1. a biochar-based cathode deriving from the pyrolysis of the organic fraction of municipal solid waste (OW) and 2. a biochar-based cathode deriving from the pyrolysis of wood chips (WC). The performance of these two biochar-cathodes was evaluated in MFC, MEC and MES configurations in terms of voltage generation, CH_4 production and production of VFA, respectively. Cathodic microbial communities for each system were further characterized to assess the main drivers of the performances achieved.

2. Materials and methods

2.1. Biochar-based electrodes preparation

Samples of the organic fraction of municipal solid waste (OW) were gathered at an Italian (Pieve Fissiraga, Lodi) biogas plant while wood chips (WC) were commercially purchased from AM CASALI (Chignolo Po, Pavia).

Both OW and WC underwent pyrolysis (600 °C under an N_2 flux for 30 min of operation time), which was conducted in a pilot-scale oven at PETROCERAMICS SPA (Kilometro Rosso, Parco Scientifico Tecnologico, Bergamo). The obtained biochar was further powdered (particle size: 20 μm).

Cathodes were constructed using 10 × 10 cm carbon cloth squares (SAATI C1, Appiano Gentile, Italy) as conductive support. A functionalizing suspension was prepared by combining 3 g of naturally doped biochar, 1 ml of polytetrafluoroethylene (PTFE) solution (60 % dispersion in water) (Sigma-Aldrich, Germany), and 60 ml of distilled water. The resulting suspension was applied to the carbon cloth and then heat-treated five times in a muffle at 340 °C for 30 min. Doing so, both rectangular (2.5 × 7 cm; with a surface area of 17.5 cm^2) and round (3.8 cm diameter; with a surface area of 10.74 cm^2) electrodes were produced using both biochar, i.e., OW and WC. Additionally, a third electrode was created as negative control (CC). This control was necessary to distinguish and investigate the effects of the biochar functionalization (i.e. OW and WC cathodes) vs. the background effect that can derive from the support (the bare carbon cloth). Therefore, this control was designed identical to the support used for the biochar-functionalized electrodes, i.e., 2.5 × 7 cm of carbon cloth, but without the biochar functionalization.

2.2. MFCs and MECs set-up and operational conditions

All MFCs and MECs experiments were conducted at 25 ± 2 °C. The electrode potential data are reported against an Ag/AgCl (3 M KCl) reference electrode.

2.2.1. Microbial fuel cells

Six single-chamber MFCs were constructed using lab-scale prototypes of plastic cubic single-chamber air-cathode MFCs with a volume of 28 mL (Fig. 1). Two replicates were carried out for each treatment (CC, WC, and OW) across the whole experiment due to the high replicability experienced previously [27,28]. Results achieved in this work confirmed this.

The anode was composed of a graphite fiber brush with a titanium wire core (Panex 33,160 K, Zoltec, US), cut to 2.5 cm in diameter and 2.5 cm in length. The surface area was estimated to be 0.22 m^2 and 95 % of the brush was porous. The round functionalized carbon cloths (cathodes) were positioned in the slightly recessed ends of the MFC, with the functionalized side facing the anode. A circular rubber gasket was then placed over the electrode to ensure a watertight seal. The MFCs were filled with wastewater samples from a wastewater treatment plant, which had been pre-acclimatized with sodium acetate (3 g L^{-1}) until the MFCs operated stably. The purpose of acclimation (~9 days) was to stimulate the growth of electroactive microorganisms initially present in the wastewater sample [29].

Subsequently, the MFCs were supplied with an artificial medium containing 3 g L^{-1} of sodium acetate. The composition of the artificial medium per liter was as follows: 982.5 mL phosphate buffer solution (NH_4Cl 0.31 g L^{-1}; $NaH_2PO_4 \bullet H_2O$ 2.452 g L^{-1}; Na_2HPO_4 4.576 g L^{-1}; KCl 0.13 g L^{-1}), 12.5 mL mineral solution and 5 mL vitamin solution. These MFCs were operated in a fed-batch mode (3 cycles of ~8 days) in a closed-circuit mode by connecting the anode and cathode with a 500 Ω external load resistance. A multichannel Data Logger (Keithley 2700 Multimeter) was connected to collect the potential of the MFCs every 30 min (Choudhury et al., 2020). Cyclic voltammetry tests were conducted in the range of 0.8 V to −0.8 V, at scan rate of 0.5 mV s^{-1} to investigate cathode (working electrode) performance and analyze electron transfers (Simoska et al., 2023).

2.2.2. Microbial electrolysis cells

Design, medium and acclimatization for the MEC were analogous to the MFC (Fig. 1); the cathode however was not exposed to air and it was covered with an acrylic lid to avoid ORR. Acclimation lasted ~9 days and after they were operated in a fed-batch mode (3 cycles, total running time after acclimation ~60 days). These cells were further adapted with the addition of a 16-mL glass cylinders, tightly sealed with a PTFE rubber cover and an aluminium crimp. The generated gas was collected in a gas-tight bag connected to the glass cylinder through a PVC hosepipe and a syringe needle.

Both electrodes were connected to a power source (ISO-TECH DC Power Supply, Merseyside, England) with an applied voltage of 800 mV. The gas composition was analyzed using gas chromatography (μGC; 3000A-μGC, AGILENT-SRA Instruments, Santa Clara, CA, USA), and the volume was measured using injection syringes.

Similarly to the MFCs, cyclic voltammetry (CV) tests were conducted under the same conditions at the cathode.

2.3. MES inoculum, set-up and operational conditions

All MESs experiments were conducted at 25 ± 2 °C. The electrode potential data are reported against an Ag/AgCl (3 mol L^{-1} KCl) reference electrode.

2.3.1. Microbial inoculum, selection and enrichment

Wastewater sludge culture, sourced from an Italian wastewater treatment plant (Peschiera Borromeo Lombardy), was used as the inoculum for enriching a chemolithoautotrophic culture.

The enrichment experiments were carried out in serum bottles (120 mL) filled with 40 mL of growth medium, based on Patil et al., 2015 (Table S-1), with a pH of 7. Additionally, 40 mL of inoculum was added.

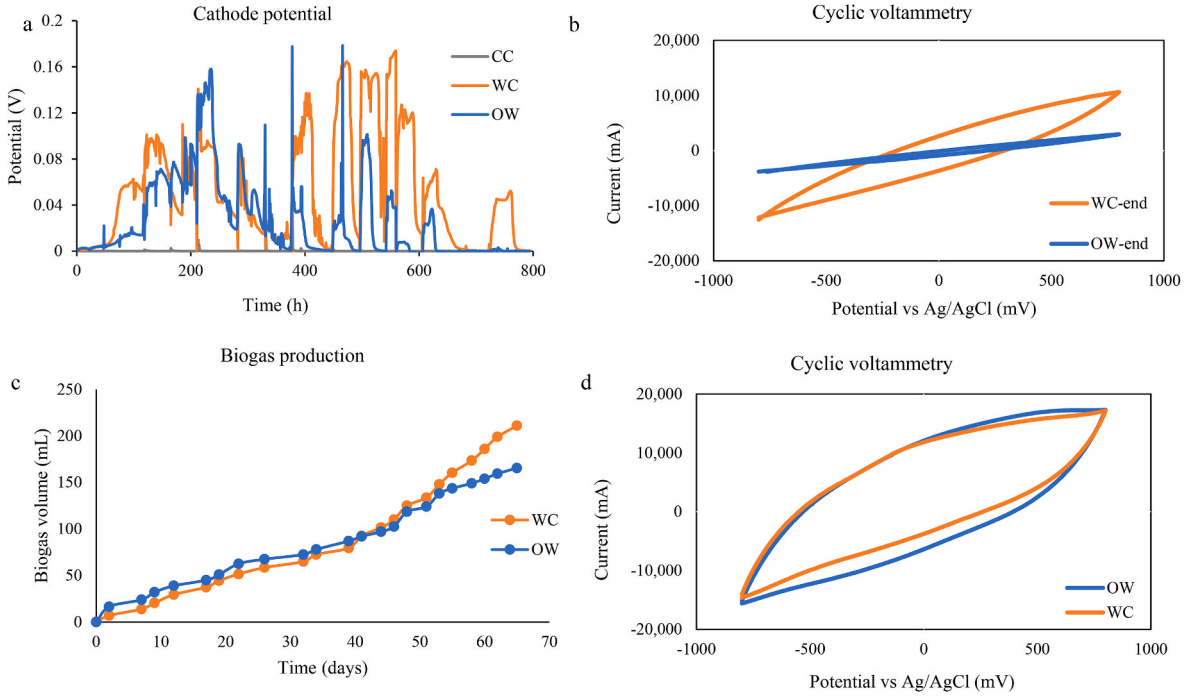

Fig. 1. Cathode potential and cyclic voltammetry of air cathode MFCs and gas volume and cyclic voltammetry in MECs. The CVs were conducted with scan rate of 0.5 mV s^{-1} in the artificial medium described in 2.2.1 Microbial Fuel Cells. a) Cathode potential of four cycle in MFCs; b) Cyclic voltammograms of woodchip (WC) and organic waste (OW) biochar-based cathodes in MFCs; c) Gas volume in MECs; d) Cyclic voltammograms of woodchip (WC) and organic waste (OW) biochar-based cathodes in MECs.

The composition of the growth medium per liter was as follows: K_2HPO_4 0.2 g L-1; NH_4Cl 0.25 g L^{-1}; KCl 0.5 g L^{-1}; $CaCl_2 \bullet 2H_2O$ 0.15 g L^{-1}; $MgCl_2 \bullet 6H_2O$ 0.6 g L^{-1}; NaCl 1.2 g L^{-1}; $NaHCO_3$ 30 mL from an 84 g L^{-1} stock; trace metal solution 1 mL; vitamin solution 2.5 mL; and tungstate-selenium solution 0.1 mL. In addition, 2-bromoethanesulfonate (2-BES) was introduced at a concentration of 0.5 g L^{-1} in the medium to inhibit the growth of methanogens.

An overpressure of 50 kPa (1.5 atm) was applied to the headspace using an H_2:CO_2 (80:20 v/v) gas mixture as the sole source of carbon and energy. Acclimation (enrichment of the CO_2-fixing mixed microbial community) was carried out for one month, and its success was confirmed through monitoring optical density (OD) (UV–VIS spectrophotometer), pH, electrical conductivity, and gas sample analysis.

The selected and enriched culture was then used as the inoculum for the microbial electrosynthesis experiment (MES) after the detection and quantification of volatile fatty acids (VFAs) by high-pressure liquid chromatography (Shimadzu HPLC, Hi-Plex H Agilent column, 300 × 7 mm, PL1170-6830, Agilent Technologies, Santa Clara, CA, USA). Prior to inoculation in the MES reactor, the feed was switched to H_2 20 % (v/v) - CO_2 80 % (v/v) for two weeks.

2.3.2. MES reactor set up and experiments with CO_2

MES experiments were conducted in six 120 mL two-chambered reactors (H-type) under a cathodic potential of −1.0 V (Ag/AgCl) using a feed of 100 % CO_2 (Fig. S1). The two different rectangular biochar-based electrodes were tested to determine the best performer as the working electrode (i.e., cathode). In the anodic chamber (counter electrode), a graphite electrode with the same area as the cathode (7 × 3.5 cm) was used. The reference electrode was an Ag/AgCl (3 M KCl) reference electrode and was placed in the cathode chamber. The anode and cathode electrodes were separated by a proton exchange membrane. Each electrode chamber had a volume of 125 mL and three ports for electrode placement and sampling purposes. The working volume of anolyte and catholyte was 100 ml, and the inoculum constituted 40 % of the catholyte. The catholyte and the anolyte were the same medium as described in section 2.2.1 with a pH of 7.

Every day, 10 mL of CO_2 was added to the reactors, serving as the only carbon source, and the reduction current response was monitored using a chronoamperometry (CA) technique. MES experiments were conducted in batch cycles by replenishing the spent medium at the end of each cycle. Liquid samples were collected at the end of each cycle for further analysis. One control experiment, inoculated but not electrically connected, thus lacking an electron source, was conducted to confirm microbially catalyzed electricity-driven bioproduction. Cyclic voltammograms (CVs) were recorded in a potential window of −1.0 and 1.0 V at a scan rate of 1 mV s^{-1} in the middle of each batch cycle.

2.4. Electrochemical analyses

2.4.1. Electrodes characterization

Dried samples of OW and WC were characterized before and after pyrolysis to assess qualitative changes that occurred during thermal processing. pH, total organic carbon (TOC), total nitrogen (TN), and mineral content, were determined using inductively coupled plasma-mass spectrometry (BRUKER Aurora-M90 ICP-MS, Bremen, Germany). Additionally, volatile and total solids were assessed by routine methodology.

Fiber distribution was determined using the neutral detergent fiber (NDF) and acid detergent fiber (ADF) methods within feed filter bags (Methods 6 and 5, respectively, ANKOM Technology, Macedon, NY, USA). Specific surface area, total volume, and pore diameter distribution for mesoporous and microporous materials were analyzed via the Brunauer, Emmett, and Teller (BET) method [30] by using a Plus Adsorption Analyzer (ASAP 2020, Micromeritics, Norcross, Georgia, USA).

Cyclic voltammetry tests were conducted to evaluate and compare the performance of OW and WC electrodes in terms of organic molecule production (Simoska et al., 2023). Furthermore, spectroscopic analysis was carried out by Fourier Transform Infrared (FT-IR). The spectra were collected in total reflectance mode (ATR) using a Shimadzu IRAffinity-1S equipped with a Miracle Pike ATR device (Shimadzu Italia Srl, Milan, Italy), covering a wavenumber range of 4000–500 cm^{-1} with a resolution of 2 cm^{-1}. Shimadzu LabSolutions IR Peak Software (Shimadzu Italia Srl, Milan, Italy) was used to process the collected FT-IR spectra.

One-way ANOVA analyses (excel) were performed to assess statistical differences.

2.4.2. BESs characterization

The liquid samples from all BES experiments were analyzed for VFA production using a Shimadzu HPLC (Shimadzu Corporation, Tokyo, Japan) equipped with a Hi-Plex H Agilent column (300 × 7 mm, PL1170-6830) (Agilent Technology, Santa Clara, CA, USA) and a 5 mmol L^{-1} H_2SO_4 mobile phase. The flow rate was set at 0.5 mL min^{-1}, and the temperature was maintained at 60 °C. Microbial growth was assessed by monitoring the optical density (OD) at 600 nm using a UV–VIS spectrophotometer (7305 Spectrophotometer, Jenway, St Neots, United Kingdom). Additionally, biomass production in MES experiments was confirmed through soluble chemical oxygen demand (COD) analysis (Rice et al., 2012).

Gas samples collected from the headspace of serum flasks were subjected to gas chromatography (μGC; 3000A-μGC, AGILENT-SRA Instruments, Santa Clara, CA, USA) for the detection of H_2, CO_2, and CH_4.

For MES products (i.e. VFAs), acetic acid titer, conversion rate per day, surface-based rate per day, and coulombic efficiency (electron recovery into products) were calculated following protocols described elsewhere (Patil et al., 2015b).

One-way ANOVA analyses (excel) were performed to assess statistical differences.

2.5. 16S rRNA gene NGS, bioinformatics and statistics

DNA extraction was performed from the inoculum and the cathodic biofilms from all BESs experiments.

DNA was extracted from each sample in technical triplicate using the DNeasy® PowerSoil® Kit (Qiagen, Germany) according to manufacturer's instructions after an initial step of thermal treatment (5 cycles of 10 min at −20 °C and 10 min at 65 °C). The yield and purity (A_{260}/A_{280} and A_{260}/A_{230}) of the extracted DNA was quantified on a Nanodrop 1000 spectrophotometer (Thermo Fisher Scientific) while eventual fragmentation was determined through gel electrophoresis 0.8 % (w/v) 1 × TAE agarose gels. DNA was stored at −80 °C until analyses. Replicates were then pooled together to minimize extraction bias.

The NGS was performed at Stab Vida Lda (Lisbon, Portugal). Sequencing targeted the V3 and V4 regions of the bacterial 16S rRNA gene using primers 341F (CCTACGGGNGGCWGCAG) and 785R (GACTACHVGGGTATCTAATCC) [31]. The generated DNA libraries were sequenced with MiSeq Reagent Kit Nano in the Illumina MiSeq platform, using 300bp paired-end sequencing reads. The nucleotide sequences generated and analyzed are available at the NCBI SRA repository (BioProject accession number: PRJNA1067882). The sequences resulting from the NGS were quality checked through the FastQC software and analyzed using DADA2 [32]. DADA2 for R was used as per https://benjjneb.github.io/dada2/tutorial.html. Reads were truncated for all analyses at 280 (forward) and 220 (reverse) in order to remove the low-quality section of the reads. The adapter sequence was further removed with the trimLeft function set at the length of the primers for both forward and reverse reads. For taxonomic assignment, the SILVA database was used.

All statistical analyses were performed on R studio (version 4.1.2) mainly with the package vegan while taxonomic summaries were performed using the phyloseq package, as by Clagnan et al. [33]. Linear Discriminant Analysis Effect Size (LEfSe) were executed as per htt

ps://usegalaxy.eu/.

3. Result and discussion

3.1. Biochar-based electrodes composition and characterization

The composition and characterization of the organic fraction of municipal solid waste (OW) and wood chips (WC), before and after pyrolysis, are summarized in Table 1. Characteristics of both OW and WC for pH, TOC, TN, TS and VS content, VS/TS, and ash, were in line with standard literature data.

OW and WC showed a carbon content of 483 ± 14 g kg^{-1} dry weight (dw) and 531 ± 42 g kg^{-1} dw, respectively, compared to an average content from literature, of 466 ± 44 g kg^{-1} dw and 500 ± 40 g kg^{-1} dw, respectively ([34]; Lamlom et al., 2003). In terms of TN content, Campuzano et al. [34] found an average content of 7.9 ± 5.4 g kg^{-1} dw for OW, while we found a content of 5.8 ± 0.9 g kg^{-1} dw. For WC, Lamlom et al. (2003) stated that the TN content in wood is generally around 1 %, which aligns with the WC TN content of this study (1.6 ± 0.4 g kg^{-1} dw). After pyrolysis, TOC and TN remained constant (Table 1), indicating that they were not significantly affected by the high-temperature treatment (5.89 ± 0.99 g kg^{-1} dw vs. 5.7 ± 0.3 g kg^{-1} dw for OW and 1.59 ± 0.45 g kg^{-1} dw vs. 1.92 ± 0.27 g kg^{-1} dw for WC, respectively, before and after pyrolysis).

On the other hand, the pH doubled, increasing from 5.19 ± 0.02 to 10.17 ± 0.03 for OW and from 5.63 ± 0.04 to 9.34 ± 0.06 for WC (Table 1). It appears that the high-temperature thermal treatment shifted the pH toward basic values.

In terms of fiber content, pyrolysis significantly reduced both cellulose and hemicellulose content of both OW and WC (Table 1). Conversely, the lignin content increased to 603 ± 21 g kg^{-1} for OW and 530 ± 16 g kg^{-1} for WC, starting from initial content of 101 ± 2 g kg^{-1} and 311 ± 40 g kg^{-1}, respectively (Table 1). The initial fiber values for WC were within the expected range. Wood mass composition typically consists of approximately 25 % lignin, 45 % cellulose, and 25 % hemicelluloses [35], whereas OW is low in lignin content, as food waste is generally richer in fat, protein, cellulose, hemicellulose, starch, and free sugars [34].

ICP-MS analysis confirmed a higher content of each mineral element in OW than in WC before thermal treatment [34] (Table 1). After pyrolysis, only Cr and Ni decreased in both biochar samples, going from 0.24 ± 0.28 mg kg^{-1} to 0.09 ± 0.01 mg kg^{-1} in OW and from 0.05 ± 0.04 mg kg^{-1} to 0.04 ± 0.01 mg kg^{-1} in WC, while all the other values doubled or tripled (Table 1). Although heavy metals were present in low quantities in both biochar samples, the abundance of the remaining elements in OW biochar could potentially inhibit the bioelectrochemical system [36]. Contrarily, metals such as Fe, Al, and Zn, when present in limited quantities, for example in WC biochar, can improve electron transfer in BESs because they act as oxygen reduction catalysts [37–39]. Indeed, the use of transition metals as doping agents to improve the electrode performance is widely diffused [37–39]. The effect of metals content on BES performance is discussed in section 3.3.

The purpose of obtaining biochar from waste materials was to enhance performance in MEC, MFC, and MES experiments. A larger surface area is known to lead to better attachment of bacteria to the cathode, resulting in higher extracellular electron transfer and increased biomolecule production [40]. BET results show that the surface area for both biochar samples increased compared to the original samples, with

Table 1
Raw biomass and derived biochar characterization.

	OW	WC	OW biochar	WC biochar
pH	5.19 ± 0.02A[a,b]	5.63 ± 0.04B	10.17 ± 0.03b	9.34 ± 0.06a
Total C (g kg^{-1} dw)	483 ± 14A	531 ± 42A	573 ± 34a	686 ± 22b
Total N (g kg^{-1} dw)	5.8±1B	1.59 ± 0.45A	5.7 ± 0.3b	1.9 ± 0.3a
VS (g kg^{-1} dw)	754 ± 12A	870±9B	nd[c]	nd
TS (g kg^{-1} wet weight)	305 ± 17A	945±7B	nd	nd
VS/TS	0.75 ± 0.19A	0.9 ± 0.2A	nd	nd
ASH	772 ± 12B	57±6A	nd	nd
Cellulose (g kg^{-1}VS)	222±5A	298 ± 30B	27±6a	26±1a
Hemicellulose (g kg^{-1}VS)	135 ± 35A	154 ± 19A	20±6a	25±3a
Lignin (g kg^{-1}VS)	101±2A	311 ± 40B	603 ± 21b	530 ± 16a
Total lignocellulose (g kg^{-1}VS)	458 ± 15A	763±9B	647 ± 19b	581 ± 17a
Soluble cell material (g kg^{-1}VS)	542 ± 15B	237±9A	353 ± 19a	419 ± 17b
BET surface area (m^2 g^{-1})	0.2 ± 0.0A	5.19 ± 0.53B	1.65 ± 0.16a	7.52 ± 0.25b
Na (mg kg^{-1})	67.35 ± 4.76B	2.26 ± 1.88A	178 ± 36b	3.4 ± 2.1a
Mg (mg kg^{-1})	23.4 ± 1.8B	8.98 ± 0.84A	60 ± 15b	23.92 ± 1.92a
Al (mg kg^{-1})	25.08 ± 3.95B	0.46 ± 0.27A	58.2 ± 21.7b	0.98 ± 0.08a
K (mg kg^{-1})	120 ± 11B	41.9 ± 4.2A	371 ± 67b	89.21 ± 4.76a
Ca (mg kg^{-1})	335 ± 14B	78.32 ± 2.02A	753 ± 149b	243±7a
Cr (mg kg^{-1})	0.24 ± 0.28B	0.05 ± 0.04A	0.09 ± 0.01b	0.04 ± 0.01a
Mn (mg kg^{-1})	0.61 ± 0.08B	0.18 ± 0.02A	1.65 ± 0.13b	0.62 ± 0.01a
Fe (mg kg^{-1})	14 ± 0.11B	0.94 ± 0.02A	26.07 ± 5.91b	2.78 ± 0.23a
Ni (mg kg^{-1})	1.04 ± 1.44B	0.07 ± 0.11A	0.08 ± 0.05b	0.01 ± 0.01a
Cu (mg kg^{-1})	0.1 ± 0.03B	0.07 ± 0.03A	0.29 ± 0.01b	0.11 ± 0.03a
Zn (mg kg^{-1})	0.56 ± 0.03B	0.14 ± 0.04A	1.12 ± 0.04b	0.68 ± 0.12a
P (mg kg^{-1})	80.03 ± 10.48B	20.63 ± 2.98A	171±6b	48.96 ± 6.72a

[a] (av. ± st. dev., n = 2).
[b] Average followed by the same letter are non-statistically different (upper case for raw materials and lower case for derived biochars) (ANOVA, Tukey Test, $p < 0.05$).
[c] (nd = not detected).

Table 2
Performances of MFC experiment perfprmed using organic waste (OW)- and woody chips- (WC) biochar electrodes and carbon cloth (CC) electrodes.

	OW	WC	CC
MFC			
pH	8.10a[a]	8.27a	7.93a
Conductivity (mS cm^{-1})	8.65 ± 1.77a[b]	8.93 ± 3.29a	2.66 ± 0.49b
Maximum output voltage (mV)	100 ± 10a	200 ± 25b	–
MEC			
pH	7.2 ± 0.2a	7.2 ± 0.2a	–
Conductivity (mS cm^{-1})	12.4 ± 1.8a	12.4 ± 1.8a	–
Biogas daily production rate (mL d^{-1})	3.6 ± 0.4a	3.0 ± 0.5b	–
Total biogas volume produced (mL)	215±3a	179 ± 3.57b	–
CH_4 volume (% v/v)	73.22 ± 3.92a	70.24 ± 8.03a	–
MES			
pH	7.8 ± 0.4a	7.2 ± 0.3a	–
Conductivity (mS cm^{-1})	8.1 ± 1.3a	7.9 ± 1.6a	–
Daily acetic acid production rate (mg HA L^{-1} d^{-1})	0.03 ± 0.4a	0.3 ± 0.13b	–
COD (mg L^{-1})	73 ± 2.3a	87 ± 4.6a	–
CO_2 conversion rate in HA (mol %)	11 ± 1.3a	65 ± 2.4b	–

[a] (av. ± st. dev., n = 2).
[b] Significance is represented by lowercase letters for each row (ANOVA, Tukey Test, $p < 0.05$).

OW and WC biochar reaching values of 7.52 ± 0.25 m^2 g^{-1} and 5.19 ± 0.53 m^2 g^{-1}, respectively (Table 2). To better understand how pyrolysis affected the structure of the biomasses, various Fourier-transform infrared spectroscopy analyses were performed.

FT-IR spectra of biomasses before and after pyrolysis for OW revealed a strong peak around 3300 cm^{-1} (stretching vibration of hydrogen bond O-H), as well as two intense bands at 2920 and 2850 cm^{-1} corresponding to the C-H stretching vibration in aliphatic compounds (Fig. S2a, Table S4). These bands are typically associated with carbohydrates, polysaccharides, and lipids found in rice, meat, and vegetables characterizing OW [41–43]. The peak at 1740 cm^{-1}, indicating the stretching of the C=O bond of ester carbonyl groups, suggests the presence of pectic carbohydrates and lipid esters such as triglyceride [44,45]. Additionally, the peak at 1240 cm^{-1}, assigned to the C-N group of amides, confirms the presence of proteins [46]. The absorption bands in the 1150–900 cm^{-1} region, typically attributed to C–O stretching of polysaccharides or polysaccharide-like substances, confirmed the abundance of these compounds in OW. The presence of absorption bands at 850-750 and 750-700 cm^{-1} demonstrated the presence of N-compounds like amides and amines. The FT-IR spectra of WC exhibited main absorption bands associated with cellulose, lignin, pectin, and hemicellulose (Fig. S2b, Table S4). The bands at 3300 and 2920 cm^{-1} may be attributed to cellulose and hemicellulose. The peak at 1740 cm^{-1} (stretching of the C=O bond of carboxylic acids of ester carbonyl group) is usually assigned to pectin, while the broad peak at 1150–900 cm^{-1} (C–O stretching) is assigned to cellulose and hemicellulose. The small aromatic band at 1630 and 1510 cm^{-1}, as well as the small bands around 1400 and 1200 cm^{-1}, originate from lignin and lignocellulose. As expected, pyrolysis significantly altered the intensity and category of the chemical functional groups in the pyrolyzed biomasses (Figs. S1a, b, and c) [41]. The major changes included the complete disappearance of absorption bands at 3300, 2920, 2850, and 1150-900 cm^{-1}, suggesting that the thermal treatment decomposed hydroxyl groups, ether bonds, and aliphatic C structures associated with carbohydrates and fats. This observation aligns with Wang et al. [41], who reported a significant reduction of these absorption bands during sewage sludge pyrolysis. The thermal treatment also resulted in a strong reduction in protein content in OFMWS, leading to the disappearance of absorption bands assigned to this class of compounds in the pyrolyzed OW (1240, 850-750, and 750-700 cm^{-1}) (Fig. S2a).

On the other hand, the intensity of peaks associated with aromatic compounds, particularly lignin, in wood chips showed only slight variations (Fig. S2b), indicating that aromatic structures in biomasses were not significantly affected by pyrolysis, as previously reported in the literature [41]. The persistence of these structures may imply the formation of condensed aromatic structures in biochar, which could influence the physicochemical properties of the produced biochar.

Finally, a well-defined absorption band at 875 cm^{-1} was evident in pyrolyzed biomasses (Fig. S2c). Since the intensity of this band increased after pyrolysis in both cases, it may be associated with inorganic compounds, such as carbonates, that are not affected by thermal treatments and become more evident in the spectra due to the decomposition of organic compounds.

3.2. Performances comparison in MFC and MEC

Values are reported in Table 2 as the mean of the two replicates for each cathode material: WC biochar-based electrode, OW biochar-based electrode, and the CC electrode. pH values of a single-chamber air cathode MFC used for bioelectricity generation were obtained during the acetate feed-batch cycle for each different cathode material. Due to the proton consumption by the cathode reactions [47], the pH increased after 2 days, starting from the same value of 6.76 and reaching 7.93, 8.10, and 8.27 for CC, OW, and WC, respectively (Table 2). This pH increase occurred because anodic bacteria require a pH close to neutral for optimal growth, while oxygen reduction on the cathode electrode leads to an alkaline pH. A conventional MFC can maintain two distinct pH values to optimize anodic and cathodic processes ([48]; Kumar and Mungray, 2016). It is reported that the optimal pH for an air cathode is between 8 and 10, and as demonstrated in this experiment, the electrolyte pH stabilizes around a neutral pH after 25 days of operating time [49].

In terms of conductivity, average values of 8.93 ± 3.29 mS cm^{-1}, 8.65 ± 1.77 mS cm^{-1}, and 2.66 ± 0.49 mS cm^{-1} were reached by CC, WC, and OW, respectively, starting from the same value of 10.36 mS cm^{-1} (Table 2). The solution's conductivity determines the ion transport rate. Thus, higher conductivity enhances ionic conduction and minimizes Ohmic losses, resulting in an increase in MFC power output [50]. WC biochar showed higher current production and electron transfer rates than OW biochar, as shown in Fig. 1a.

After inoculum acclimation, the anodic open working potential (OCP) was measured every two days. Creating an anoxic environment at the anode and promoting the growth and metabolism of microorganisms on its surface led to the formation of a negative potential. For each setup, the anodic OCP responded to the feed of substrate by rapidly reaching more negative values at the beginning of each cycle, and then stabilizing along the cycle duration, suggesting that bacterial growth and metabolism are associated with substrate refreshment [51,52].

About voltage generation, after the acclimation period and steady operation over three cycles, the variation in the output voltage of MFCs with different biochar-based cathodes was plotted in Fig. 1a. At the beginning of the pre-acclimation cycle, the bacteria began to proliferate and degrade the organic substrate; at this point, OW and WC performances are comparable. After ~400 h, the difference between WC and OW in voltage generation became relevant: the WC produced double the amount of electricity compared to OW, reaching a maximum output voltage of over 200 mV, while for OW, it was half that (100 mV) (Table 2). A typical observed open-circuit voltage (OCV) of an air–cathode MFC is in the range of 200–500 mV [53]. The drop between each cycle was due to the depletion of sodium acetate and, consequently, electrolyte replacement. Cyclic voltammetry analyses were performed at the beginning and end of the whole experimental running time (acclimation excluded). In Fig. 1b, cyclic voltammograms measured at the cathode of WC and OW are reported. Cyclic voltammetry (CV) is a method used in electrochemistry that, among other things, allows the observation of the effect that biofilms attached to anode and/or cathode electrodes have [54]. Different biocatalytic capabilities and biofilm stage developments are reflected in the various shapes and patterns obtained from the compared electrodes throughout the whole experimental running time (acclimation excluded). Comparing the results at the end of the operation period, at the cathode, the current values recorded in the cyclic voltammograms of WC electrodes was higher compared to OW electrodes, indicating higher electrochemical activity of the WC electrode.

In the MEC experiments, pH was periodically monitored along with conductivity. Starting from a value of 6.7, pHs reached neutral value (7.2 ± 0.2) during MEC runs, with this pH being optimal for the growth of methanogenic bacteria or bacteria in which the methane metabolic pathway is dominant [55] (Table 2). The initial conductivity value, corresponding to the feeding solution, was around 10.36 mS cm^{-1}, while the final conductivity value reached 12.4 ± 1.8 mS cm^{-1} (Table 2). Open working potential (OCP) was measured on the anodic and cathodic MEC electrodes during the feed-batch cycles period. By creating an anoxic environment at the anode and promoting the growth and metabolism of microorganisms on its surface, a negative potential was produced. The anodic OCP responded to the feed of substrate by quickly reaching more negative values at the beginning of each cycle and then stabilizing along the cycle duration due to the applied voltage (800 mV), which suggests that bacterial growth and metabolism are associated with the replenishment of substrate, as in previous MFC experiments [51,52].

CV analyses were applied to describe the oxidation-reduction

reactions on the electrode surface by measuring the current response at the electrode surface in an unstirred solution.

The anode, cathode, and Ag/AgCl electrode acted as the working electrode, counter electrode, and reference electrode, respectively. In Fig. 1d, the CV profiles of both WC and OW biochars at the end of the experiments in MEC are represented. From the CV analysis, no evident differences can be noted between the WC and OW cathode voltammograms.

As previously stated, the WC-based cathode showed better performances in CVs, but also in both the amount of biogas produced and composition. The WC biochar set-up produced 215 ± 3 mL in 60 days (3.6 mL per day) of biogas with a higher methane percentage (73.22 ± 3.92 % v/v), while the biogas generated by the OW biochar set-up was lower in terms of quantity (179 ± 3.57 mL, 3.0 mL per day) and methane concentration (70.24 ± 8.03 % v/v) (Table 2, Fig. 1c). In an experiment by Jiang et al. [56], the same reaction was performed (cathodic potential −0.85 to −1.15 V vs. Ag/AgCl) using a cathode made of carbon felt with an area of 49 cm^2, resulting in an 80.9 mL per day of methane production.

3.3. Performances comparison in MES

VFAs detection was used as the indicator of bacterial natural efficiency in converting CO_2 into organic compounds using H_2 as source of electrons. After a selection and enrichment process and ensuring the presence of VFAs, which were initially present in low concentrations (below 0.1 g L^{-1}), the selected bacteria were inoculated into the MES reactor. During the serum bottle experiment, pH and conductivity remained stable. The working temperature was approximately 25 ± 2 °C.

pH and conductivity were periodically measured in both setups. Conductivity values were similar: 8.2 ± 1.3 mS cm^{-1} was found in OW reactors, while in WC, it was 8.1 ± 1.3 mS cm^{-1} (Table 2). pH values were also similar, around 7.8 at the cathodes and 2.1 in the anodes.

Although BET analysis suggests that OW should be a better electrode than WC due to its larger surface area, cyclic voltammetry results do not confirm this (Fig. 2c). Considering cyclic voltammetry at the end of the experiment (after two months), Fig. 2c shows a steeper slope and a broader curve shape in the WC setup compared to the OW experiment, where the curve is almost flat. This indicates that in the WC setup, a reduction reaction occurred, while in the OW setup, no significant reactions (reductions or oxidations) were detected.

Indeed, it was found that 11 ± 1.3 % of CO_2 moles sparged during the feeding were converted into acetic acid every day, while the total conversion yield reached 65 ± 2.4 % in the WC reactor (Table 2). The relationship between soluble COD and acetic acid production rate showed an equal biomass content in both samples but a concentration of acetic acid 10 times higher in WC (0.3 ± 0.13 g L^{-1} d^{-1}) than in OW (0.03 ± 0.4 g L^{-1} d^{-1}) over two months (Table 2, Fig. 2).

Experiments with a standard graphite-felt electrode and inoculum from a wastewater treatment plant achieved lower results in acetic acid production (0.139 g L^{-1} d^{-1}) than that reported in this work, with a potential applied of −0.8 V (Bajracharya et al., 2017b). Contrarily, higher results (1.04 g L^{-1} d^{-1}) were obtained with an inoculum from an adapted brewery sludge with an applied potential of 0.590 V [57]. WC-based electrodes should be tested in future experiments with variations in parameters such as the applied potential or the inoculum used.

In a paper by Zi-Ai Xu et al. (2022), it was found that a surface-activated natural wood biomass electrode was very efficient in MES, possibly due to its 2D (carbon cloth)-3D (biochar) hybrid structure, which provided a high surface area and multiple transportation pathways. This structure attracted more bacterial cells and facilitated the interfacial electron transfer between cells and the electrode. Authors also found that the WC-based electrode produced 3.1 times higher

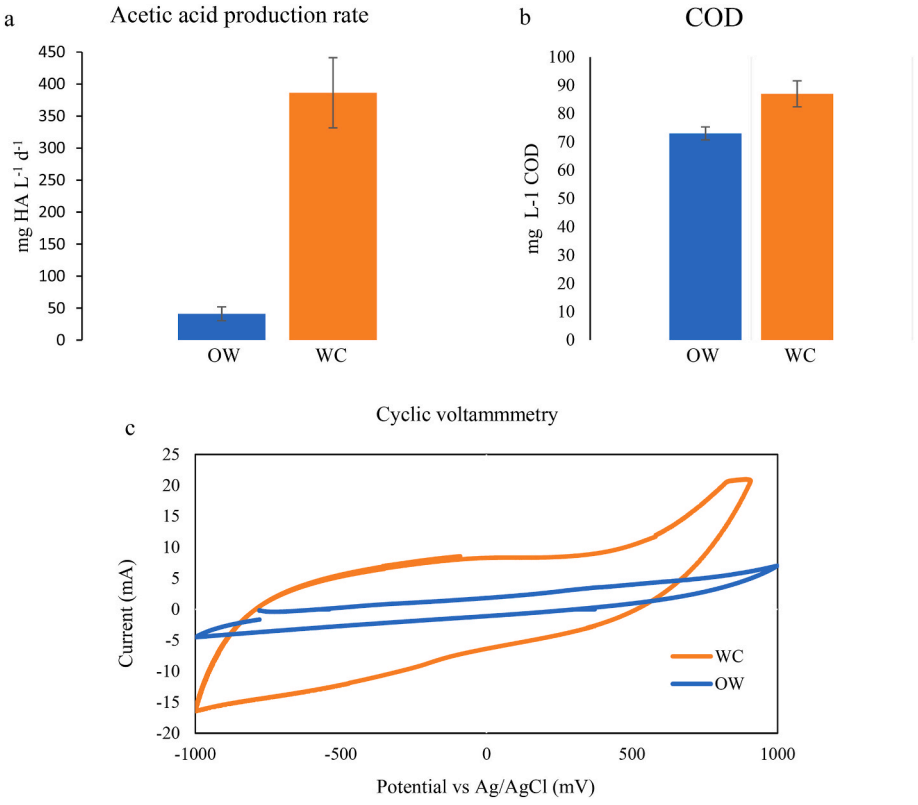

Fig. 2. Histograms of acid (HA) in MES system (a); COD concentration (mg L d^{-1}) of woodchip (WC) and organic waste (OW) biochar-based cathodes (b). Cyclic voltammograms of woodchip (WC) and organic waste (OW) biochar-based cathodes in MES systems (c). The CVs were conducted with scan rate of 1 mV s^{-1} in the artificial medium described in 2.2.1 Microbial Fuel Cells.

formic acid (3.3 mmol L^{-1} vs 0.8 mmol L^{-1}) and 8.3 times higher power output (483 mW m^{-2} vs 52 mW m^{-2}) than the conventional carbon cloth electrode. In this case, the biochar was produced from natural wood and then activated by hydrothermal treatment and pyrolysis.

In conclusion, it can be said that wood-chip biochar works better as an electrode than the organic fraction of municipal solid waste biochar. It is possible that some compounds present in the latter act as inhibitors for CO_2 conversion into VFAs in microbial electrosynthesis.

Regarding the effect of heavy and transition metal contents in the biochar, it seemed that they were not affecting the electrode performance, as the best performing electrode was the WC that contained a very limited metal amount with respect to OW electrode (Table 1). These results suggested that probably the biochar structure (i.e. graphite-like structure of WC biochar) rather than the metal contents most affected the BES performance.

3.4. Microbial community

Due to the different working set up and the low number of cycles, MESs cells were not able to produce a high amount of microbial biomass and therefore the total retrieved DNA was too low to proceed with the NGS analysis. The microbial characterization was therefore focused on the inoculum and the MFC and MEC systems.

The 16S rRNA gene NGS produced between 84,469 and 173,949 reads while between 35,970 and 86,507 reads passed the trimming, assembling and removal of chimeras steps (Table S2).

All systems led to a reduction in the observed richness (number of amplicon sequence variants (ASVs)) when compared to the inoculum, possibly due to a specialization of the community (Table S3). MEC showed the highest diversity for WC when compared to both CC and OW while for MFC all cathodes were similar. In terms of both Shannon's and Simpson's diversity index and of the Pielou's evenness the same pattern was seen with highest values for the inoculum; the other two systems showed similar values across the three different cathodes, and were generally higher for MFCs than MECs.

In terms of phylum most samples were characterized by the presence of Bacteroidota and Proteobacteria (Fig. S3), which are phyla largely populated by electrogenic organisms [58]. The inoculum was further enriched in Chloroflexi, Myxococcota, Patescibacteria, Planctomycetota and Verrucomicrobiota. Both MFC and MEC systems were characterized

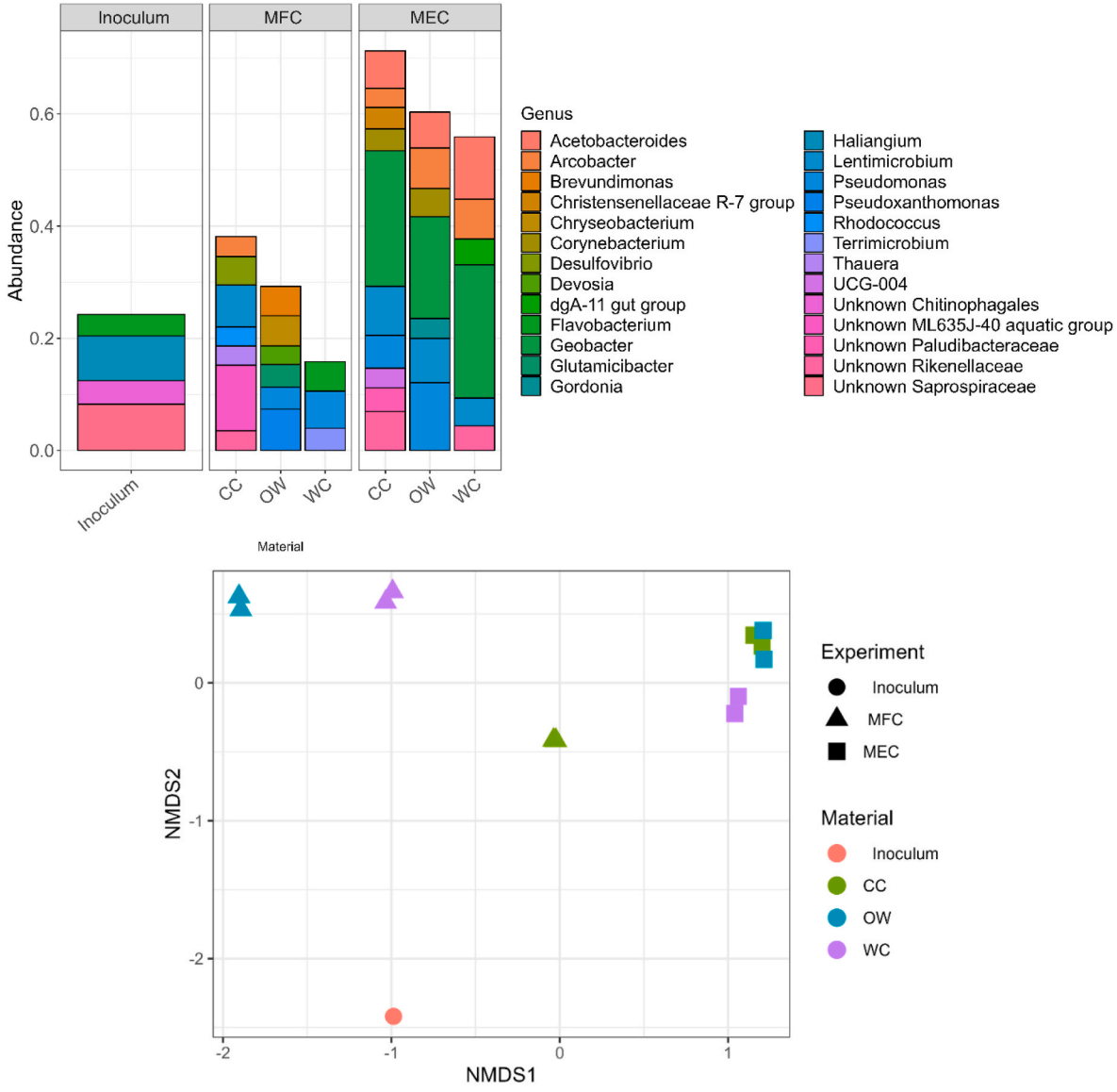

Fig. 3. Prokaryotic communities' composition at genus level with a >2 % cut-off. Linear discriminant analysis (LDA) effect size analysis (LEfSe) at genus level for the prokaryotic communities.

by a high abundance of Actinobacteriota and Firmicutes often present in electrogenic systems and fuel cells inoculated with wastewaters [59]. MFCs showed an enrichment in Patescibacteria and Verrucomicrobiota while the MECs systems were enriched in Desulfobacterota, and Campylobacterota. Patescibacteria growth is stimulated by an electric field environment [60] while Verrucomicrobiota have been often found in BES utilized for NO_3^- removal [61]. On the other hand, Desulfobacterota are known for the breakdown of organic material followed by transportation of electrons, therefore generating current [62].

When looking at genera structure, both systems evolved and differentiated from the inoculum structures: MFC samples showed a higher variability across treatments than MEC, with its control showing a more similar structure to all MEC samples (Fig. 3).

Most abundant genera for the inoculum were Unknown Saprospiraceae (average abundance: 8.2 %), *Haliangium* (8.0 %), a genus known for producing antifungal molecules [63], unknown Chitinophagales (4.2 %) and *Flavobacterium* (3.8 %).

The MFC system showed a different array of most abundant genera across the three treatments: CC was characterized by a high abundance of *Lentimicrobium* (7.5 %), *Desulfovibrio* (5.1 %), *Arcobacter* (3.6 %), *Thauera* (3.4 %) and *Rhodococcus* (3.4 %). *Lentimicrobium* is a genus of strictly anaerobic fermentative bacteria also playing an important role in substrate degradation in MFCs [64]. *Desulfovibrio*, *Arcobacter* and *Rhodococcus* contribute to both electricity generation and, together with *Thauera*, organics degradation [28,64,65].

The OW cathode showed an abundance of *Pseudoxanthomonas* (7.4 %), *Chryseobacterium* (5.4 %); a chemoorganotroph, *Brevundimonas* (5.2 %), *Glutamicibacter* (4.0 %), *Pseudomonas* (3.9 %) and *Devosia* (3.3 %). Both *Pseudomonas* and *Pseudoxanthomonas* were previously found in MFCs systems, they are involved in carbon and nitrogen degradation and electron generation overall improving MFCs' performance where high N is present [66]. *Glutamicibacter* was found in MFCs and linked to ammonia oxidation [67] while *Devosia* is linked to denitrification [68].

The WC cathode, similarly to OW, was characterized by *Pseudomonas* (6.6 %) together with *Flavobacterium* (5.2 %), which has been mainly linked to electrogenesis and, similarly to *Terrimicrobium* (4.0 %), to organics degradation [22,69].

The MEC system showed a higher similarity of the most abundant genera across the three cathodes. The CC cathode showed a high abundance of *Geobacter* (24 %), *Lentimicrobium* (8.7 %), *Acetobacteroides* (6.7 %), *Pseudomonas* (5.9 %), *Corynebacterium* (3.9 %), *Christensenellaceae R-7 group* (3.8 %), *UCG-004* (3.5 %) and *Arcobacter* (3.5 %). *Geobacter* is a typical electricity-generating microbe which has been shown to boost hydrogen and methane production efficiency of other microorganisms linked to fermentative electrotrophy [70]. *Acetobacteroides* is a fermentative bacterium and hydrogen producer [71]. *Corynebacterium* is another electrogenic bacterium and protein producer [72] while *Christensenellaceae* R-7 group and *UCG-004* have links with electron transfer and electroactivity [73,74].

Similarly, the OW cathode was characterized by *Geobacter* (18 %), *Pseudomonas* (12 %), *Lentimicrobium* (7.8 %), *Arcobacter* (7.2 %), *Acetobacteroides* (6.4 %), *Corynebacterium* (5.0 %) and *Gordonia* (3.6 %) another electrogenic bacterium that degrades hydrocarbons [75].

The same set of genera was again maintained for WC: *Geobacter* (24 %), *Acetobacteroides* (11 %), *Arcobacter* (7.1 %), *Lentimicrobium* (4.9 %) and dgA-11 gut group (4.4 %). These bacteria, found at high abundance, show a further significant enrichment within the MEC reactors according to a LefSE analysis that was further carried out to highlight differentially enriched genera between the two cathodes (OW vs. WC) and between the two systems (MEC vs MFC) (Fig. S4).

4. Conclusion

In the present study, two biochar-based cathodes were tested and compared in MFC, MEC, and MES systems for energy and biomolecules production. Wood chips biochar-based cathodes exhibited better performances both in MFC and MEC set-ups. In MFC, they excelled in terms of current production, electron transfer rate, voltage generation, and consequently in electricity generation. In MEC, both biogas production and methane content were higher compared to the OW biochar-based cathodes. Concerning MES, a significantly higher concentration of acetic acid (10 times more) was found in the MES setup with woody chips biochar thanks to the higher BET values and its carbonaceous graphite-like structure. In summary, it can be seen that the raw biomass of ligno-cellulosic waste, after pyrolysis, presented a carbonaceous structure similar to graphite, with well-aligned rings that make up the carbonaceous structure. This alignment allows for greater electron flow on the cathode surface, which in turn has been colonized by electroactive bacteria. These bacteria use the cathode to produce electricity, methane, or catalyze VFAs. In contrast, biochar produced from organic waste has a less organized and linear carbon structure, which does not facilitate easy electron flow. Future studies will focus on scaling up the process and increasing the TRL, while aiming to maintain the performance rates mentioned above.

CRediT authorship contribution statement

Andrea Goglio: Writing – original draft, Investigation, Data curation, Conceptualization. **Arianna Carrara:** Writing – original draft, Investigation. **Hager Galal Elsayed Elboghdady:** Writing – original draft, Formal analysis. **Mirko Cucina:** Writing – original draft, Formal analysis, Data curation. **Elisa Clagnan:** Methodology, Formal analysis, Data curation, Conceptualization. **Gabriele Soggia:** Writing – review & editing, Data curation. **Patrizia De Nisi:** Investigation, Formal analysis. **Fabrizio Adani:** Writing – original draft, Supervision, Funding acquisition, Data curation, Conceptualization.

Declaration of competing interest

The authors declare that they have no known competing financial interests or personal relationships that could have appeared to influence the work reported in this paper.

Acknowledgements

This study was carried out within the Agritech National Research Center and received funding from the European Union Next-Generation EU (PIANO NAZIONALE DI RIPRESA E RESILIENZA (PNRR) – MISSIONE 4 COMPONENTE 2, INVESTIMENTO 1.4 – D.D. 1032 June 17, 2022, CN00000022). This manuscript reflects only the authors' views and opinions, neither the European Union nor the European Commission can be considered responsible for them.

Appendix A. Supplementary data

Supplementary data to this article can be found online at https://doi.org/10.1016/j.jpowsour.2024.235623.

Data availability

No data was used for the research described in the article.

References

[1] S.S. Hassan, G.A. Williams, A.K. Jaiswal, Moving towards the second generation of lignocellulosic biorefineries in the EU: drivers, challenges, and opportunities, Renew. Sustain. Energy Rev. 101 (2019) 590–599, https://doi.org/10.1016/j.rser.2018.11.041.

[2] N. Hajilary, M. Rezakazemi, CFD modeling of CO2 capture by water-based nanofluids using hollow fiber membrane contactor, Int. J. Greenh. Gas Control 77 (2018) 88–95, https://doi.org/10.1016/j.ijggc.2018.08.002.

[3] V. Masson-Delmotte, P. Zhai, H.-O. Pörtner, D. Roberts, J. Skea, P.R. Shukla, A. Pirani, W. Moufouma-Okia, C. Péan, R. Pidcock, S. Connors, J.B.R. Matthews, Y. Chen, X. Zhou, M.I. Gomis, E. Lonnoy, T. Maycock, M. Tignor, T. Waterfield,

IPCC, 2018: global Warming of 1.5°C. An IPCC Special Report on the impacts of global warming of 1.5°C above pre-industrial levels and related global greenhouse gas emission pathways, in: The Context of Strengthening the Global Response to the Threat of Climate Change, Sustainable Development, and Efforts to Eradicate Poverty, Cambridge University Press, Cambridge, UK and New York, NY, USA, 2019, https://doi.org/10.1017/9781009157940.
[4] M. Younas, M. Rezakazemi, M. Daud, M.B. Wazir, S. Ahmad, N. Ullah, Inamuddin, S. Ramakrishna, Recent progress and remaining challenges in post-combustion CO2 capture using metal-organic frameworks (MOFs), Prog. Energy Combust. Sci. 80 (2020) 100849, https://doi.org/10.1016/j.pecs.2020.100849.
[5] NOAA National Centers for Environmental Information, State of the climate: global climate report for annual, published online January 2021, retrieved on February 1, 2022 from, https://www.ncdc.noaa.gov/sotc/global/202013, 2020. (Accessed 19 September 2023).
[6] A.I. Stefanakis, C.S. Calheiros, I. Nikolaou, Nature-based solutions as a tool in the new circular economic model for climate change adaptation, Circ. Econ. Sust. 1 (2021) 303–318, https://doi.org/10.1007/s43615-021-00022-3.
[7] T. Trainer, Some problems in storing renewable energy, Energy Pol. 110 (2017) 386–393, https://doi.org/10.1016/j.enpol.2017.07.061.
[8] I.N. Pulidindi, A. Gedanken, The catalytic production of biofuels (biodiesel and bioethanol) using sonochemical, microwave, and mechanical methods, in: B. Torok, C. Schaefer (Eds.), Nontraditional Activation Methods in Green and Sustainable Applications, Elsevier, 2021, pp. 171–239, https://doi.org/10.1016/B978-0-12-819009-8.00013-X.
[9] A. Muscat, E.M. de Olde, I.J.M. de Boer, R. Ripoll-Bosch, The battle for biomass: a systematic review of food-feed-fuel competition, Global Food Secur. 25 (2020) 100330, https://doi.org/10.1016/j.gfs.2019.100330.
[10] K. Rabaey, R. Rozendal, Microbial electrosynthesis — revisiting the electrical route for microbial production, Nat. Rev. Microbiol. 8 (2010) 706–716, https://doi.org/10.1038/nrmicro2422.
[11] H. Wang, Z.J. Ren, A comprehensive review of microbial electrochemical systems as a platform technology, Biotechnol. Adv. 31 (8) (2013) 1796–1807, https://doi.org/10.1016/j.biotechadv.2013.10.001.
[12] D.R. Lovley, K.P. Nevin, A shift in the current: new applications and concepts for microbe-electrode electron exchange, Curr. Opin. Biotechnol. 22 (3) (2011) 441–448, https://doi.org/10.1016/j.copbio.2011.01.009.
[13] M.I. San-Martín, D. Leicester, E. Heidrich, R. Alonso, R. Mateos, A. Escapa, Bioelectrochemical systems for energy valorization of waste streams, in: P. Tsvetkov (Ed.), Energy Systems and Environment, IntechOpen, 2018, https://doi.org/10.5772/intechopen.74039.
[14] R. Dey, D. Maarisetty, S.S. Baral, A comparative study of bioelectrochemical systems with established anaerobic/aerobic processes, Biomass Convers. Biorefin. 1–16 (2022), https://doi.org/10.1007/s13399-021-02258-3.
[15] B. Bian, S. Bajracharya, J. Xu, D. Pant, P.E. Saikaly, Microbial electrosynthesis from CO2: challenges, opportunities and perspectives in the context of circular bioeconomy, Bioresour. Technol. 302 (2020) 122863, https://doi.org/10.1016/j.biortech.2020.122863.
[16] J.E. Dykstra, A. ter Heijne, S. Puig, P.M. Biesheuvel, Theory of transport and recovery in microbial electrosynthesis of acetate from CO2, Electrochim. Acta 379 (2021) 138029, https://doi.org/10.1016/j.electacta.2021.138029.
[17] K.P. Nevin, T.L. Woodard, A.E. Franks, Z.M. Summers, D.R. Lovley, Microbial electrosynthesis: feeding microbes electricity to convert carbon dioxide and water to multicarbon extracellular organic compounds, mBio 1 (2) (2010) e00103, https://doi.org/10.1128/mBio.00103-10, 10.
[18] D.A. Jadhav, S.G. Ray, M.M. Ghangrekar, Third generation in bio-electrochemical system research–A systematic review on mechanisms for recovery of valuable by-products from wastewater, Renew. Sust. Energ. Rev. 76 (2017) 1022–1031, https://doi.org/10.1016/j.rser.2017.03.096.
[19] M.T. Noori, G.D. Bhowmick, B.R. Tiwari, M.M. Ghangrekar, C.K. Mukhrejee, Application of low-cost Cu–Sn bimetal alloy as oxygen reduction reaction catalyst for improving performance of the microbial fuel cell, MRS Advances 3 (2018) 663–668, https://doi.org/10.1557/adv.2018.163.
[20] S. Marzorati, A. Goglio, S. Fest-Santini, D. Mombelli, F. Villa, P. Cristiani, A. Schievano, Air-breathing bio-cathodes based on electro-active biochar from pyrolysis of Giant Cane stalks, Int. J. Hydrogen Energy (2018), https://doi.org/10.1016/j.ijhydene.2018.07.167.
[21] A. Schievano, R. Berenguer, A. Goglio, S. Bocchi, S. Marzorati, L. Rago, R.O. Louro, C.M. Paquete, A. Esteve-Núñez, Electroactive biochar for large-scale environmental applications of microbial electrochemistry, ACS Sustain. Chem. Eng. (2019), https://doi.org/10.1021/acssuschemeng.9b04229.
[22] W. Chen, J. Huang, J. Wei, D. Zhou, J. Cai, H. Zhengda, Y. Chen, Origins of high onset overpotential of oxygen reduction reaction at Pt-based electrocatalysts: a mini review, Electrochem. Commun. 96 (2018) 71–76, https://doi.org/10.1016/j.elecom.2018.09.011.
[23] S.K. Bhatia, A.K. Palai, A. Kumar, R.K. Bhatia, A.K. Patel, V.K. Thakur, Y.H. Yang, Trends in renewable energy production employing biomass-based biochar, Bioresour. Technol. 340 (2021) 125644, https://doi.org/10.1016/j.biortech.2021.125644.
[24] S. Li, S.-H. Ho, T. Hua, Q. Zhou, F. Li, J. Tang, Sustainable biochar as an electrocatalysts for the oxygen reduction reaction in microbial fuel cells, Green Energy Environ. 6 (5) (2021) 644–659, https://doi.org/10.1016/j.gee.2020.11.010.
[25] N. Aryal, F. Ammam, S.A. Patil, D. Pant, An overview of cathode materials for microbial electrosynthesis of chemicals from carbon dioxide, Green Chem. 19 (2017) 5748–5760, https://doi.org/10.1039/C7GC01801K.
[26] S. Li, C. Cheng, A. Thomas, Carbon-based microbial-fuel-cell electrodes, Adv. Mater. 29 (8) (2017), https://doi.org/10.1002/adma.201602547.
[27] G. Ghiara, S. Campisi, A. Goglio, F. Formicola, M. Balordi, A. Gervasini, S.P. M. Trasatti, F. Adani, A. Franzetti, P. Cristiani, Biochar based cathode enriched with hydroxyapatite and Cu nanoparticles boosting electromethanogenesis, Sustain. Energy Technol. Assessments 57 (2023) 103274, https://doi.org/10.1016/j.seta.2023.103274.
[28] M. Gualtieri, A. Goglio, E. Clagnan, F. Adani, The importance of the electron acceptor: comparison between flooded and tidal bioelectrochemical systems for wastewater treatment and nutrients enriched solution production, Bioresour. Technol. Rep. 24 (2023) 101617, https://doi.org/10.1016/j.biteb.2023.101617.
[29] L. Tian, X. Yan, D. Wang, Q. Du, Q. Wan, L. Zhou, T. Li, C. Liao, N. Li, X. Wang, Two key Geobacter species of wastewater-enriched electroactive biofilm respond differently to electric field, Water Res. 213 (2022) 118185, https://doi.org/10.1016/j.watres.2022.118185.
[30] S. Brunauer, P.H. Emmett, E. Teller, Adsorption of gases in multimolecular layers, J. Am. Chem. Soc. 60 (1938) 309–319, https://doi.org/10.1021/ja01269a023.
[31] A. Klindworth, E. Pruesse, T. Schweer, J. Peplies, C. Quast, M. Horn, F.O. Glöckner, Evaluation of general 16S ribosomal RNA gene PCR primers for classical and next-generation sequencing-based diversity studies, Nucleic Acids Res. 41 (1) (2013) e1, https://doi.org/10.1093/nar/gks808.
[32] B.J. Callahan, P.J. McMurdie, M.J. Rosen, A.W. Han, A.J.A. Johnson, S.P. Holmes, High-resolution sample inference from Illumina amplicon data, Nat. Methods 13 (2016) 581–583, https://doi.org/10.1038/nmeth.3869.
[33] E. Clagnan, G. D'Imporzano, M. Dell'Orto, A. Sanchez-Zurano, F.G. Acién-Fernandez, B. Pietrangeli, F. Adani, Profiling microalgal cultures growing on municipal wastewater and fertilizer media in raceway photobioreactors, Bioresour. Technol. 360 (2022) 127619, https://doi.org/10.1016/j.biortech.2022.127619.
[34] R. Campuzano, S. González-Martínez, Characteristics of the organic fraction of municipal solid waste and methane production: a review, Waste Manag. 54 (2016) 3–12, https://doi.org/10.1016/j.wasman.2016.05.016.
[35] E. Sjostrom, Wood Chemistry—Fundamentals and Applications, Academic Press, San Diego, 1993.
[36] B. Hemdan, V.K. Garlapati, S. Sharma, S. Bhadra, S. Maddirala, K.M. Varsha, V. Motru, P. Goswami, S. Sevda, T.M. Aminabhavi, Bioelectrochemical systems-based metal recovery: resource, conservation and recycling of metallic industrial effluents, Environ. Res. 204 (2022) 112346, https://doi.org/10.1016/j.envres.2021.112346.
[37] Y. Pan, X. Mo, K. Li, L. Pu, D. Liu, T. Yang, Iron–nitrogen–activated carbon as cathode catalyst to improve the power generation of single-chamber air-cathode microbial fuel cells, Bioresour. Technol. 206 (2016) 285–289, https://doi.org/10.1016/j.biortech.2016.01.112.
[38] H. Tang, Y. Zeng, Y. Zeng, R. Wang, S. Cai, C. Liao, H. Cao, X. Lu, P. Tsiakara, Iron-embedded nitrogen doped carbon frameworks as robust catalyst for oxygen reduction reaction in microbial fuel cells, Appl. Catal. B Environ. 202 (2017) 550–556, https://doi.org/10.1016/j.apcatb.2016.09.062.
[39] P. Song, M. Luo, X. Liu, W. Xing, W. Xu, Z. Jiang, L. Gu, Zn single atom catalyst for highly efficient oxygen reduction reaction, Adv. Funct. Mater. 27 (2017) 1700802, https://doi.org/10.1002/adfm.201700802.
[40] L. Chen, W. Fang, J. Chang, J. Liang, P. Zhang, G. Zhang, Improvement of direct interspecies electron transfer via adding conductive materials in anaerobic digestion: mechanisms, performances, and challenges, Front. Microbiol. 13 (2022) 860749, https://doi.org/10.3389/fmicb.2022.860749.
[41] X. Wang, V. Wei-Chung Chang, Z. Li, Z. Chen, Y. Wang, Co-pyrolysis of sewage sludge and organic fractions of municipal solid waste: synergistic effects on biochar properties and the environmental risk of heavy metals, J. Hazard Mater. 412 (2021) 125200, https://doi.org/10.1016/j.jhazmat.2021.125200.
[42] N. Mlaik, S. Khoufi, M. Hamza, M.A. Masmoudi, S. Sayadi, Enzymatic pre-hydrolysis of organic fraction of municipal solid waste to enhance anaerobic digestion, Biomass Bioenergy 127 (2019) 105286, https://doi.org/10.1016/j.biombioe.2019.105286.
[43] E. Smidt, K. Meissl, The applicability of Fourier transform infrared (FT-IR) spectroscopy in waste management, Waste Manag. 27 (2) (2007) 268–276, https://doi.org/10.1016/j.wasman.2006.01.016.
[44] A. Borba, A. Gomez-Zavaglia, Infrared spectroscopy: an underexploited analytical tool for assessing physicochemical properties of food products and processing, Curr. Opin. Food Sci. 49 (2023) 100953, https://doi.org/10.1016/j.cofs.2022.100953.
[45] T. Hong, J. Yin, S. Nie, M. Xie, Applications of infrared spectroscopy in polysaccharide structural analysis: progress, challenge and perspective, Food Chem. X 12 (2021) 100168, https://doi.org/10.1016/j.fochx.2021.100168.
[46] N.B. Yahmed, H. Carrere, M.N. Marzouki, I. Smaali, Enhancement of biogas production from Ulva sp. by using solid-state fermentation as biological pretreatment, Algal Res. 27 (2017) 206–214, https://doi.org/10.1016/j.algal.2017.09.005.
[47] F. Zhao, F. Harnisch, U. Schröder, F. Scholz, P. Bogdanoff, I. Herrmann, Challenges and constraints of using oxygen cathodes in microbial fuel cells, Environ. Sci. Technol. 40 (17) (2006) 5193–5199, https://doi.org/10.1021/es060332p.
[48] s. Bagchi, M. Behera, Evaluation of the effect of anolyte recirculation and anolyte pH on the performance of a microbial fuel cell employing ceramic separator, Process Biochem. 102 (2021) 207–221, https://doi.org/10.1016/j.procbio.2021.01.008.
[49] Z. He, Y. Huang, A.K. Manohar, F. Mansfeld, Effect of electrolyte pH on the rate of the anodic and cathodic reactions in an air-cathode microbial fuel cell, Bioelectrochemistry 74 (1) (2008) 78–82, https://doi.org/10.1016/j.bioelechem.2008.07.007.

[50] S. Gadkari, J.-M. Fontmorin, E. Yu, J. Sadhukhan, Influence of temperature and other system parameters on microbial fuel cell performance: numerical and experimental investigation, J. Chem. Eng. 388 (2020) 124176, https://doi.org/10.1016/j.cej.2020.124176.
[51] S. Marzorati, A. Schievano, A. Colombo, G. Lucchini, P. Cristiani, Ligno-cellulosic materials as air-water separators in low-tech microbial fuel cells for nutrients recovery, J. Clean. Prod. 170 (2018) 1167–1176, https://doi.org/10.1016/j.jclepro.2017.09.142.
[52] M.M. Mardanpour, M. Nasr Esfahany, T. Behzad, R. Sedaqatvand, Single chamber microbial fuel cell with spiral anode for dairy wastewater treatment, Biosens. Bioelectron. 38 (1) (2012) 264–269, https://doi.org/10.1016/j.bios.2012.05.046.
[53] N.J. Koffi, S. Okabe, High voltage generation from wastewater by microbial fuel cells equipped with a newly designed low voltage booster multiplier (LVBM), Sci. Rep. 10 (2020) 18985, https://doi.org/10.1038/s41598-020-75916-7.
[54] S.V. Ramanaiah, C.M. Cordas, S. Matias, L.P. Fonseca, In situ electrochemical characterization of a microbial fuel cell biocathode running on wastewater, Catalysts 11 (7) (2021) 839, https://doi.org/10.3390/catal11070839.
[55] S.K. Foad Marashi, H.R. Kariminia, Performance of a single chamber microbial fuel cell at different organic loads and pH values using purified terephthalic acid wastewater, J. Environ. Health Sci. Eng. 13 (1) (2015) 1–6, https://doi.org/10.1186/s40201-015-0179-x.
[56] Y. Jiang, M. Su, Y. Zhang, G. Zhan, Y. Tao, D. Li, Bioelectrochemical systems for simultaneously production of methane and acetate from carbon dioxide at relatively high rate, Int. J. Hydrogen Energy 38 (8) (2013) 3497–3502, https://doi.org/10.1016/j.ijhydene.2012.12.107.
[57] C.W. Marshall, D.E. Ross, E.B. Fichot, R.S. Norman, H.D. May, Long-term operation of microbial electrosynthesis systems improves acetate production by autotrophic microbiomes, Environ. Sci. Technol. 47 (11) (2013) 6023–6029, https://doi.org/10.1021/es400341b.
[58] M. Burns, M. Qin, Ammonia recovery from organic nitrogen in synthetic dairy manure with a microbial fuel cell, Chemosphere 325 (2023) 138388, https://doi.org/10.1016/j.chemosphere.2023.138388.
[59] Y.P. Afsharian, M. Rahimnejad, Functional dynamics of microbial communities in bioelectrochemical systems: the importance of eco-electrogenic treatment of complex substrates, Curr. Opin. Electrochem. 31 (2022) 100816, https://doi.org/10.1016/j.coelec.2021.100816.
[60] Z. Cheng, D. Xu, Q. Zhang, Z. Tao, R. Hong, Y. Chen, X. Tang, S. Zeng, S. Wang, Enhanced nickel removal and synchronous bioelectricity generation based on substrate types in microbial fuel cell coupled with constructed wetland: performance and microbial response, Environ. Sci. Pollut. Res. 30 (2023) 19725–19736, https://doi.org/10.1007/s11356-022-23458-y.
[61] S.S. Gadegaonkar, U. Mander, M. Espenberg, A state-of-the-art review and guidelines for enhancing nitrate removal in bio-electrochemical systems (BES), J. Water Process Eng. 53 (2023) 103788, https://doi.org/10.1016/j.jwpe.2023.103788.
[62] M. Abadikhah, M. Liu, F. Persson, B.M. Wilén, A. Farewell, J. Sun, O. Modin, Effect of anode material and dispersal limitation on the performance and biofilm community in microbial electrolysis cells, Biofilms 6 (2023) 100161, https://doi.org/10.1016/j.bioflm.2023.100161.
[63] W.A. Ansari, M. Kumar, R. Krishna, A. Singh, M.T. Zeyad, P. Tiwari, S.C. Kumar, H. Chakdar, A.K. Srivastava, Influence of rice-wheat and sugarcane-wheat rotations on microbial diversity and plant growth promoting bacteria: insights from high-throughput sequencing and soil analysis, Microbiol. Res. 278 (2024) 127533, https://doi.org/10.1016/j.micres.2023.127533.
[64] Y. Zhou, S. Zhao, L. Yin, J. Zhang, Y. Bao, H. Shi, Development of a novel membrane-less microbial fuel cell (ML-MFC) with a sandwiched nitrifying chamber for efficient wastewater treatment, Electroanalysis 30 (9) (2018) 2145–2152, https://doi.org/10.1002/elan.201800232.
[65] H. Hassan, B. Jin, E. Donner, S. Vasileiadis, C. Saint, S. Dai, Microbial community and bioelectrochemical activities in MFC for degrading phenol and producing electricity: microbial consortia could make differences, J. Chem. Eng. 332 (2018) 647–657, https://doi.org/10.1016/j.cej.2017.09.114.
[66] N. Yang, H. Luo, M. Liu, X. Xiong, X. Jin, G. Zhan, Coupling mixotrophic denitrification and electroactive anodic nitrification by nitrate addition for promoting current generation and nitrogen removal, Sci. Total Environ. 856 (1) (2023) 159082, https://doi.org/10.1016/j.scitotenv.2022.159082.
[67] J. Li, S. Lin, Y. Zhang, T. Wang, H. Luo, G. Liu, Nitrogen removal with the physiological stratification of cathodic biofilm in air-cathode single-chamber microbial fuel cell under different external resistances, Chem. Eng. Sci. 275 (2023) 118746, https://doi.org/10.1016/j.ces.2023.118746.
[68] Y. Ren, Y. Lv, Y. Wang, X. Li, Effect of heterotrophic anodic denitrification on anolyte pH control and bioelectricity generation enhancement of bufferless microbial fuel cells, Chemosphere 257 (2020) 127251, https://doi.org/10.1016/j.chemosphere.2020.127251.
[69] S.-H. Liu, S.-S. You, C.-W. Lin, Y.-S. Cheng, Optimizing biochar and conductive carbon black composites as cathode catalysts for microbial fuel cells to improve isopropanol removal and power generation, Renew. Energy 199 (2022) 1318–1328, https://doi.org/10.1016/j.renene.2022.09.069.
[70] Y. A Zhang, S. Zheng, Q. Hao, O. Wang, F. Liu, Respiratory electrogen Geobacter boosts hydrogen production efficiency of fermentative electrotroph Clostridium pasteurianum, J. Chem. Eng. 456 (2023) 141069, https://doi.org/10.1016/j.cej.2022.141069.
[71] W. Guo, X. Ying, N. Zhao, S. Yu, X. Zhang, H. Feng, Y. Zhang, H. Yu, Interspecies electron transfer between Geobacter and denitrifying bacteria for nitrogen removal in bioelectrochemical system, J. Chem. Eng. 455 (2) (2023) 139821, https://doi.org/10.1016/j.cej.2022.139821.
[72] A.S. Deval, H.A. Parikh, A. Kadier, K. Chandrasekhar, A.M. Bhagwat, A.K. Dikshit, Sequential microbial activities mediated bioelectricity production from distillery wastewater using bio-electrochemical system with simultaneous waste remediation, Int. J. Hydrogen Energy 42 (2) (2017) 1130–1141, https://doi.org/10.1016/j.ijhydene.2016.11.114.
[73] Q. Yang, N. Zhao, H. Wang, B. Huang, Q. Yan, Electrochemical and biochemical profiling of the enhanced hydrogenotrophic denitrification through cathode strengthening using bioelectrochemical system (BES), J. Chem. Eng. 381 (2020) 122686, https://doi.org/10.1016/j.cej.2019.122686.
[74] L. Rago, S. Zecchin, S. Marzorati, A. Goglio, L. Cavalca, P. Cristiani, A. Schievano, A study of microbial communities on terracotta separator and on biocathode of air breathing microbial fuel cells, Bioelectrochemistry 120 (2018) 18–26, https://doi.org/10.1016/j.bioelechem.2017.11.005.
[75] T.G. Ambaye, F. Formicola, S. Sbaffoni, C. Milanese, A. Franzetti, M. Vaccari, Effect of biochar on petroleum hydrocarbon degradation and energy production in microbial electrochemical treatment, J. Environ. Chem. Eng. 11 (5) (2023) 110817, https://doi.org/10.1016/j.jece.2023.110817.